

1 **Molecular and macromolecular fractions of geological ambers**
2 **detected by evolved gas analysis-mass spectrometry**

3 Marco Mattonai*¹, Lucia Andrei¹, Marian Vîrgolici², Erika Ribechini¹

4 ¹ Department of Chemistry and Industrial Chemistry, University of Pisa, Via Giuseppe Moruzzi 13,
5 56124 Pisa, Italy

6 ² “Horia Hulubei” National Institute of Physics and Nuclear Engineering, 30, Reactorului Street,
7 Magurele, Ilfov, Romania

8

9 *Corresponding author. E-mail: marco.mattonai@dcc.unipi.it

10

11

12 **ABSTRACT**

13 We used evolved gas analysis-mass spectrometry (EGA-MS) to characterize a pool of ambers belonging
14 to different geological varieties, ~~including ambers from central Italy which were not studied by mass~~
15 ~~spectrometric methods before~~, with the aim ~~to obtain~~ of obtaining information on both their ~~molecular~~
16 ~~and macromolecular fractions~~ non-polymeric and polymeric components. Small molecular
17 components can be trapped in amber during the fossilization process. Their characterization can
18 provide insights into the maturation process of amber and help in determining its age and botanical
19 origin. Most of the analyzed ambers showed two gas evolution regions, corresponding to the
20 desorption of low-molecular weight compounds at low temperature, and to the pyrolysis of the
21 macromolecular matrix at high temperature. We established characteristic *m/z* signals of the
22 ~~molecular and macromolecular~~ non-polymeric and polymeric fractions, ~~useful to differentiate ambers,~~
23 and ~~we were able to classify most of the samples in agreement with the available literature.~~ We also
24 performed principal component analysis of diterpenoid ambers using their average mass spectra. This
25 allowed us to differentiate between succinite and rumanite ambers, which showed ~~apparently~~ very
26 similar spectra. Ambers from central Italy were also successfully ~~ca~~haracterized as diterpenoid ambers
27 containing free ~~mono- and diterpenoids~~ tetrahydro- and octahydronaphthalenes and a poly-labdane
28 polymeric network. The results demonstrate that EGA-MS constitutes a fast and reliable technique to
29 obtain information on the molecular composition of ambers, and on their relative content of low- and
30 high-molecular weight fractions.

31

32 **Keywords:** Amber; evolved gas analysis; mass spectrometry; terpenoids; succinite

33

34

1. INTRODUCTION

Amber is obtained by the fossilization of tree resin on a geological time scale. The fossilization process requires the resin to be incorporated in sediments under specific environmental conditions, such as a low availability of oxygen and closeness to a river delta or lagoon [1]. Such conditions can only be met in few places on the planet, making amber a rare, precious material whose value has been

acknowledged since ancient times [2-4]. Fossilization of tree-resin into amber is a complex phenomenon which involves two main processes: polymerization and maturation [5,6].

Polymerization involves the coupling of resin terpenoids, leading to the formation of the bulk macromolecular matrix of amber. This process is relatively fast, and can be even observed in fresh tree resin exposed to air and light. On the other hand, maturation is a slow process which involves isomerization and loss of functional groups [7]. Maturation depends not only on the composition of amber, but also on its geological age and thermal history [8].

As the macromolecular bulk of amber is formed and undergoes maturation, smaller, non-polymeric components of resin can either be lost in the environment, or trapped in the polymeric matrix. In the last decades, studies have shown that ambers at more advanced stages of maturation usually have a lower content of non-polymeric species [7]. Therefore, knowledge of the relative content of the two fractions could provide valuable insights into the degree of maturation of amber, as well as into the reaction pathways involved in the fossilization process. One of the main challenges in obtaining separate information on the molecular and macromolecular fractions of ambers is that they often share similar structural features, as the components of the non-polymeric fraction are the precursors of the polymeric one [9].

Common analytical techniques used to characterize amber are spectroscopies such as FTIR, Raman and NMR [10-13], and thermo-analytical techniques such as TGA and DSC [14,15]. However, these techniques are used to characterize whole amber samples, and separating the contributions of the molecular and polymeric fractions is extremely challenging. The non-polymeric fraction of amber can be solubilized and characterized by derivatization followed by GC-MS analysis [16] or by SPME [17]. However, this approach can be time-consuming, and often requires considerable amounts of

62 sample, which are not always available. Analytical pyrolysis coupled to GC-MS (Py-GC/MS) is a
63 powerful and widely used technique to characterize amber, providing molecular-level information on
64 both the molecular and macromolecular fractions. ~~Py-GC/MS is often carried out using *In situ*~~
65 ~~derivatization with a methylating or a silylating agent to improve the chromatographic performances~~
66 ~~of desorption/pyrolysis products with polar moieties~~ [3,7,18-22]. The pioneering work by Anderson
67 and co-workers with ~~this technique~~ Py-GC/MS led to the establishment of a well-known classification
68 system in which ambers are categorized on the basis of the structure of their polymeric fraction [6].
69 Pyrolysis temperature in Py-GC-/MS experiments can be modulated to either desorb the non-
70 polymeric components and leave the polymeric matrix unaltered, or to pyrolyze the macromolecular
71 bulk [23]. ~~While this could constitute a promising approach for the separate characterization of the~~
72 ~~two fractions of amber, very few applications are available in the literature.~~ For instance, Anderson
73 and co-workers reported that Py-GC/MS of succinite at different temperatures provided
74 chromatograms containing different sets of terpenoid compounds [18]. Virgolíci and co-workers
75 characterized amber by thermal desorption-GC/MS, heating the samples at 200 °C to desorb non-
76 polymeric compounds without degrading the macromolecular bulk [24].
77 ~~In addition, ambers~~ Ambers with different terpenoid compositions can show significantly different
78 thermal behaviors. Establishing the optimal temperature to selectively achieve desorption or pyrolysis
79 through Py-GC/MS requires preliminary studies, which can be very ~~time-consuming~~ time-intensive
80 and consume significant amounts of sample.
81 Evolved gas analysis-mass spectrometry (EGA-MS) is a ~~fast and~~ versatile technique that can be used to
82 monitor the evolution of desorption/pyrolysis products from a sample as a function of temperature.
83 EGA-MS ~~shares the advantage of Py-GC/MS of minimal sample preparation, and~~ is often used to study
84 ~~of~~ complex samples of both natural and synthetic origin, ~~and~~. EGA-MS is also a powerful screening
85 technique to establish the optimal desorption/pyrolysis temperatures before Py-GC/MS analysis [25-
86 28], ~~avoiding the need of preliminary Py-GC/MS experiments at different temperatures.~~ To the best of
87 our knowledge, however, no studies are available in the literature describing the thermal behavior of
88 ambers using EGA-MS.

89 In the present work, we performed EGA-MS of a pool of geological ambers with different origins, with
90 the aim of obtaining insights into the composition of both the ~~molecular~~ non-polymeric and polymeric
91 fractions of amber and into their thermal behaviors. ~~Three ambers collected in central Italy are also~~
92 ~~analyzed here for the first time with a mass spectrometric method.~~

93

94 2. MATERIALS AND METHODS

95 **2.1 Samples.** 46 samples of geological amber were investigated in this study. A list of all samples
96 is provided in **Table 1** Simetite is a characteristic amber deriving from a deposit close to river Simeto,
97 in Sicily, which has been dated to Miocene [14]. ~~Ambers from central Italy have been dated to~~
98 ~~Oligocene [31].~~ Information on the geological origin was not available for some of the samples. Before
99 analysis, a small amount of each sample was grinded to a fine powder using a Pulverisette 23
100 laboratory scale ball mill (Fritsch, Germany). ~~Cryo-milling with liquid nitrogen was not necessary, as~~
101 ~~all samples could be easily milled in less than 10 s, and no significant increase in temperature was~~
102 ~~observed.~~

103 **2.2 Evolved gas analysis-mass spectrometry (EGA-MS).** Experiments were performed with an
104 EGA/PY-3030D microfurnace pyrolyzer (Frontier Laboratories, Japan) coupled to a 6890 gas
105 chromatograph and a 5973 mass spectrometric detector (Agilent Technologies, USA). In each
106 experiment, approximately 100 µg of sample were directly weighted in the sample holder and inserted
107 in the pyrolysis furnace. The temperature of the furnace was then raised from 50 °C to 700 °C at 10
108 °C/min. The temperature of the pyrolysis interface was kept 100 °C above the furnace temperature, up
109 to a maximum of 300 °C. Injection was performed in split mode at 280 °C with a 20:1 ratio.
110 Desorption/pyrolysis products are directly sent to the MS detector through an UADTM-2.5N
111 deactivated stainless steel capillary tube (Frontier Laboratories, Japan) at 300 °C. Helium (1 mL min⁻¹)
112 was used as carrier gas. The mass spectrometer was operated in EI positive mode (70 eV). ~~The~~
113 ~~observed m/z range was 50 – 800}. Values below m/z 50 are generally poorly diagnostic, and their~~
114 ~~detection was avoided.~~ The ion source and quadrupole analyzer were at 230 °C and 150 °C,
115 respectively.

116 **2.3 Data processing.** EGA-MS profiles were processed with MassHunter (ver. 10.0, Agilent
117 Technologies, USA). Mass spectra were interpreted by comparison with those available in reference
118 libraries (NIST20, NIST, USA) and in previous publications [8,18,32-39]. Reproducibility of the EGA-MS
119 experiments was assessed by repeating the analysis of the same sample three times and calculating
120 the error on the total integrated area of the thermograms divided by the sample weight. The relative
121 standard deviation was 9% on average.

122 Principal component analysis (PCA) of succinite, rumanite, gedanite and gedano-succinite samples was
123 performed with OriginPro 2018. The data matrix was built with the average mass spectra of all
124 samples calculated through the whole thermal degradation range. For this data matrix, the *m/z* range
125 was restricted to 50–350 to avoid contribution from the background noise. Two additional PCAs were
126 performed using the average mass spectra calculated in two different temperature ranges: 50–300 °C
127 for the ~~molecular~~ non-polymeric components, and 300–550 °C for the polymeric components.

128 Principal components were always calculated using the covariance matrix.

129

130

131 **Table 1.** The samples were provided by nine different collections belonging to **European**
132 museums and academic institutes. ~~Classification and geographical origins for all samples were taken~~
133 ~~as available by the curators of all collections.~~ Information on the classification and geographical origins
134 of the samples are listed as provided by the institutes, when available. Eight samples derive from the
135 amber deposit in Bitterfeld, the largest amber reservoir in Germany. Bitterfeld ambers have been
136 dated to the Oligocene period, between 25 and 23 million years ago [12,16,29]. Three samples derive
137 from different locations of the Pomeranian Voivodeship, including Gdansk and Mikoszewo. Ambers
138 from the Baltic shores have also been dated to either Eocene or Oligocene [14,30]. All rumanite
139 samples derive from the basins in Colti and Pătârlagele in Romania, which are dated to Oligocene [17].
140 Simetite is a characteristic amber deriving from a deposit close to river Simeto, in Sicily, which has
141 been dated to Miocene [14]. **Ambers from central Italy have been dated to Oligocene [31].** Information
142 on the geological origin was not available for some of the samples. Before analysis, a small amount of
143 each sample was grinded to a fine powder using a Pulverisette 23 laboratory scale ball mill (Fritsch,
144 Germany). **Cryo-milling with liquid nitrogen was not necessary, as all samples could be easily milled in**
145 **less than 10 s, and no significant increase in temperature was observed.**

146 **2.2 Evolved gas analysis-mass spectrometry (EGA-MS).** Experiments were performed with an
147 EGA/PY-3030D microfurnace pyrolyzer (Frontier Laboratories, Japan) coupled to a 6890 gas
148 chromatograph and a 5973 mass spectrometric detector (Agilent Technologies, USA). In each
149 experiment, approximately 100 µg of sample were directly weighted in the sample holder and inserted
150 in the pyrolysis furnace. The temperature of the furnace was then raised from 50 °C to 700 °C at 10
151 °C/min. The temperature of the pyrolysis interface was kept 100 °C above the furnace temperature, up
152 to a maximum of 300 °C. Injection was performed in split mode at 280 °C with a 20:1 ratio.
153 Desorption/pyrolysis products are directly sent to the MS detector through an UADTM-2.5N
154 deactivated stainless steel capillary tube (Frontier Laboratories, Japan) at 300 °C. Helium (1 mL min⁻¹)
155 was used as carrier gas. The mass spectrometer was operated in EI positive mode (70 eV). **The**
156 **observed m/z range was 50 – 800}. Values below m/z 50 are generally poorly diagnostic, and their**

157 **detection was avoided.** The ion source and quadrupole analyzer were at 230 °C and 150 °C,
158 respectively.

159 **2.3 Data processing.** EGA-MS profiles were processed with MassHunter (ver. 10.0, Agilent
160 Technologies, USA). Mass spectra were interpreted by comparison with those available in reference
161 libraries (NIST20, NIST, USA) and in previous publications [8,18,32-39]. Reproducibility of the EGA-MS
162 experiments was assessed by repeating the analysis of the same sample three times and calculating
163 the error on the total integrated area of the thermograms divided by the sample weight. The relative
164 standard deviation was 9% on average.

165 Principal component analysis (PCA) **of succinite, rumanite, gedanite and gedano-succinite samples** was
166 performed with OriginPro 2018. The data matrix was built with the average mass spectra of all
167 samples calculated through the whole thermal degradation range. For this data matrix, the *m/z* range
168 was restricted to 50–350 to avoid contribution from the background noise. Two additional PCAs were
169 performed using the average mass spectra calculated in two different temperature ranges: 50–300 °C
170 for the **molecular non-polymeric** components, and 300–550 °C for the polymeric components.
171 Principal components were always calculated using the covariance matrix.

172

173

174 **Table 1.** Labels, geological **classification**, **geographical** origins, and providers of all amber samples. 1 –
 175 Natural History Museum of Warszawa, Poland; 2 – Natural History Museum of Milano, Italy; 3 – The
 176 Louvre Museum in Paris, France; 4 – Getty Institute, Los Angeles, USA; 5 – University of Padova, Italy; 6
 177 – Natural History Museum of Calci, Italy; 7 – University of Modena and Reggio Emilia, Italy; 8 – “G.
 178 Zannato” Museum of Archaeology and Natural Sciences, Montecchio Maggiore, Italy; 9 – Romanian
 179 National History Museum, Bucharest, Romania.

Label	Provider	Classification	Geographical origin	Aspect
Sg01	1	Siegburgite	Bitterfeld, Germany	
Gl01	1	Glessite	Hoyerwerda, Germany	
Gl02	1	Glessite	Not provided	
Gl03	1	Glessite	Not provided	
Ge01	1	Gedanite	Bitterfeld, Germany	
Ge02	1	Gedanite	Mikoszewo, Poland	
GS01	1	Gedano-succinite	Pomerania, Poland	
Go01	1	Goitschite	Bitterfeld, Germany	
Go02	1	Goitschite	Not provided	
BA01	1	Black amber	Bitterfeld, Germany	
BA02	1	Black amber	Bitterfeld, Germany	
BA03	1	Black amber	Ukraine	
BA04	1	Black amber	Poland	
Su01	1	Succinite	Bitterfeld, Germany	
Su02	1	Succinite	Bitterfeld, Germany	
Su03	1	Succinite	Klesow, Ukraine	
Su04	1	Succinite	Klesow, Ukraine	
Su05	1	Succinite	Jantarnyj, Russia	
Su06	2	Succinite	Not provided	
Su07	2	Succinite	Not provided	
Su08	2	Succinite	Not provided	
Su09	2	Succinite	Not provided	
Su10	2	Succinite	Not provided	
Su11	3	Succinite	Not provided	
Su12	3	Succinite	Not provided	
Su13	3	Succinite	Not provided	
Su14	3	Succinite	Not provided	
Su15	4	Succinite	Not provided	
Su16	4	Succinite	Not provided	
Su17	5	Succinite	Russia	
Su18	5	Succinite	Gdańsk – Stogi, Poland	
Su19	5	Succinite	Bitterfeld, Germany	
CI01	6	Unknown	Scannello, Italy	
CI02	7	Unknown	Loiano, Italy	
CI03	7	Unknown	Prignano, Italy	
Si01	8	Simetite	Sicily, Italy	
Si02	8	Simetite	Sicily, Italy	
Ru01	9	Rumanite	Colți, Romania	
Ru02	9	Rumanite	Colți – Pătârlagele, Romania	
Ru03	9	Rumanite	Colți – Pătârlagele, Romania	
Ru04	9	Rumanite	Colți – Pătârlagele, Romania	
Ru05	9	Rumanite	Colți – Pătârlagele, Romania	
Ru06	9	Rumanite	Sibiciu de Jos, Romania	
Ru07	9	Rumanite	Colți – Pătârlagele, Romania	
Ru08	9	Rumanite	Colți – Buzău, Romania	
Ru09	9	Rumanite	Colți – Buzău, Romania	

180

181

182 3. RESULTS AND DISCUSSION

183 3.1 Glessites and goitschites. EGA-MS profiles of a representative glessite and goitschite and

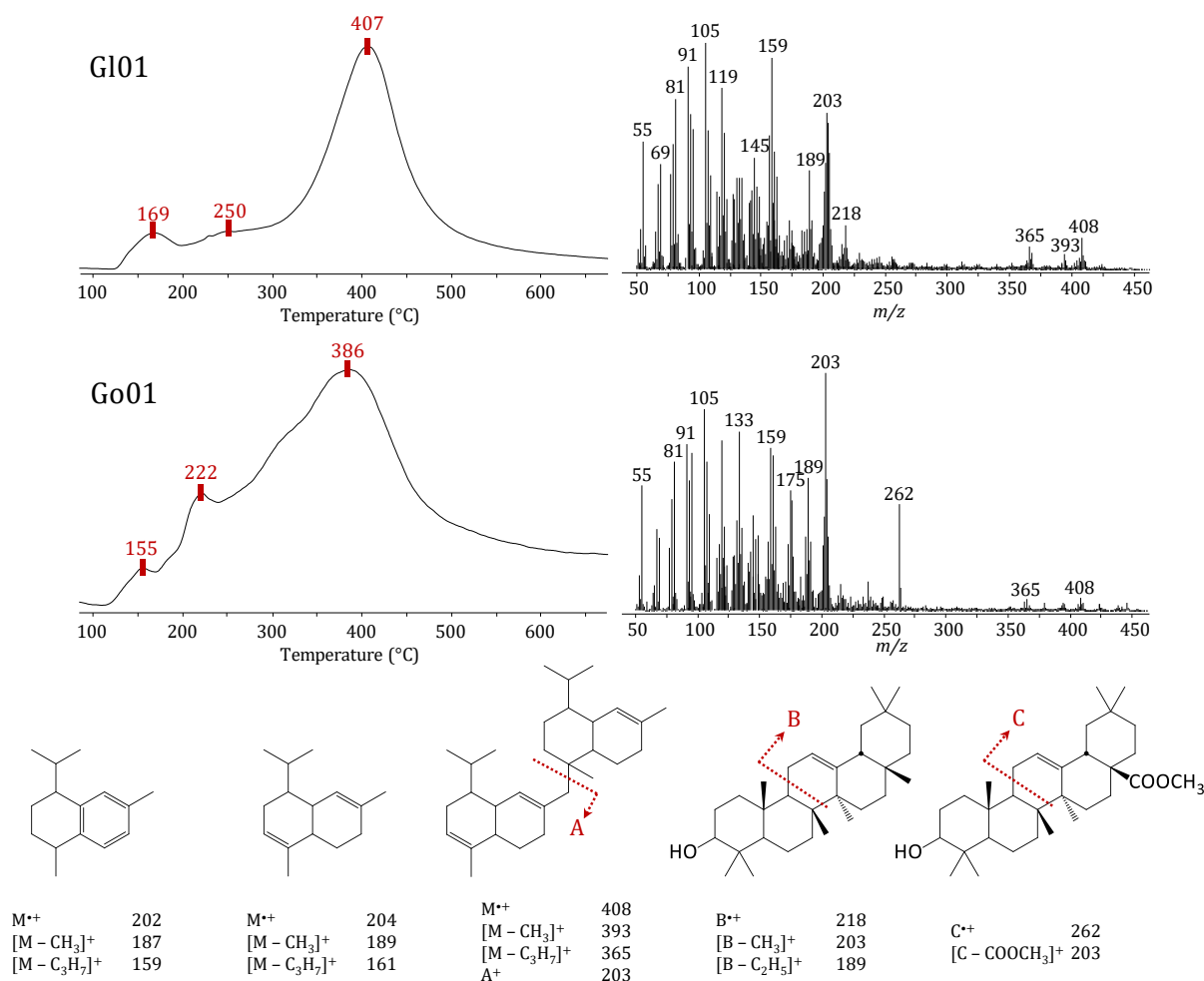
184 corresponding average mass spectra are shown in **Figure 1**, along with proposed structures for the
185 main m/z signals ~~in the average mass spectra~~. EGA-MS profiles of all samples are available in the
186 Supplementary Material. The two amber types displayed similar thermal and mass spectral features.
187 We identified three main gas evolution regions in all Gl and Go samples (see **Table 1** for compound
188 labels): a first region between 100 and 200 °C, a second region between 200 and 300 °C, and a third
189 region between 300 and 550 °C. The third region showed the highest signal intensity in all samples.
190 High signals at m/z 202 and 204 were detected in all three regions of the thermograms. These signals
191 can be ascribed to sesquiterpenoids. Sesquiterpenoids with cadinene-like structures were previously
192 identified in glessite samples by Yamamoto et al. [16]. The main MS fragmentations for cadinenes are
193 the loss of the methyl or the isopropyl group, generating the signals at m/z 161, 159, 189, and 187.
194 The signal at m/z 408 can be ascribed to dimeric cadinene. The dimer undergoes the same MS
195 fragmentations of the monomer, with loss of methyl or isopropyl groups giving m/z 365 and 393.
196 Cleavage of the C-C bond between the two sesquiterpene units is also possible, generating m/z 203.
197 The signal at m/z 203 can be observed in both the second and third region of the thermogram,
198 indicating that higher cadinene oligomers and polymers are also present in Gl and Go samples.
199 Oligomeric and polymeric cadinenes have been observed in both fresh and fossil triterpenoid resins
200 [34,40].
201 Additional signals were detected in the mass spectra of the second and third regions. Glessite samples
202 showed high intensity of m/z 218, while goitschite samples showed high intensity of m/z 262. The
203 even values indicate that the corresponding structures are obtained by rearrangement reactions. The
204 most common rearrangement in terpenes is the retro-Diels-Alder (RDA) elimination. The formation of
205 ions with m/z 218 and 262 through RDA of triterpenes has been documented in the ~~historic~~ papers by
206 Djerassi and co-workers [32,33]. As triterpenes were detected in previous studies of glessites [16], we
207 hypothesize that triterpenes are also present in our glessites and goitschites. The different m/z values
208 indicate that Gl and Go samples contain triterpenoids with different structures. In particular, m/z 218

209 can be ascribed to triterpene hydrocarbons with the ursane and oleanane structures, such as α - and β -
210 amyrin, while m/z 262 can be obtained from the methyl carboxylate equivalents of the same
211 compounds. Note that additional MS fragmentations of these ion radicals can also generate m/z 189
212 and 203, as suggested in **Figure 1**.

213 The trends of the discussed m/z signals in the three gas evolution regions can be used to outline a
214 general picture of the thermal behavior of Gl and Go ambers. The two amber types contain both
215 monomeric and oligo/polymeric sesquiterpenes, most likely with the cadinene carbon skeleton. In
216 addition, glessites also contain amyrin-like triterpenoids, while goitschites contain triterpenoids with
217 ursane or oleanane structures bearing a methyl-carboxylate functional group, most likely located on
218 carbon 28. These results allow us to ~~attribute identify~~ both Gl and Go ambers ~~to~~ as class II ambers ~~of~~
219 ~~the Anderson classification system~~ [6].

220 The results obtained for goitschites in this study are in disagreement with those of the study by
221 Yamamoto and co-workers [16], which reported the presence of diterpenoids in a goitschite sample
222 with the same geographical origin as sample Go01. This significant difference in results highlights ~~one~~
223 ~~of the main problems in amber classification: amber samples are often named after the mining sites~~
224 ~~from which they are excavated, and not on the basis of their molecular features. Therefore, ambers~~
225 ~~with very different botanical origin can often share the same geological denomination. that the~~
226 ~~geological denomination of an amber sample should always be supported by information on its~~
227 ~~molecular composition. Different results obtained from the characterization of ambers with the same~~
228 ~~geological name are not necessarily ascribable to poorly conducted experiments or mislabeling of the~~
229 ~~samples. Rather, geological denomination of amber samples is often based on their geographical origin~~
230 ~~or physical and optical features, without information on its molecular composition. This is especially~~
231 ~~true for amber samples which entered museum and academic collections in the previous century,~~
232 ~~when instrumental analytical techniques were far less available.~~

233



234

235 **Figure 1:** EGA-MS profiles and average mass spectra for samples G101 (glessite) and Go01 (goitschite).

236 Proposed structures of ions for m/z signals of relevance are also shown.

237

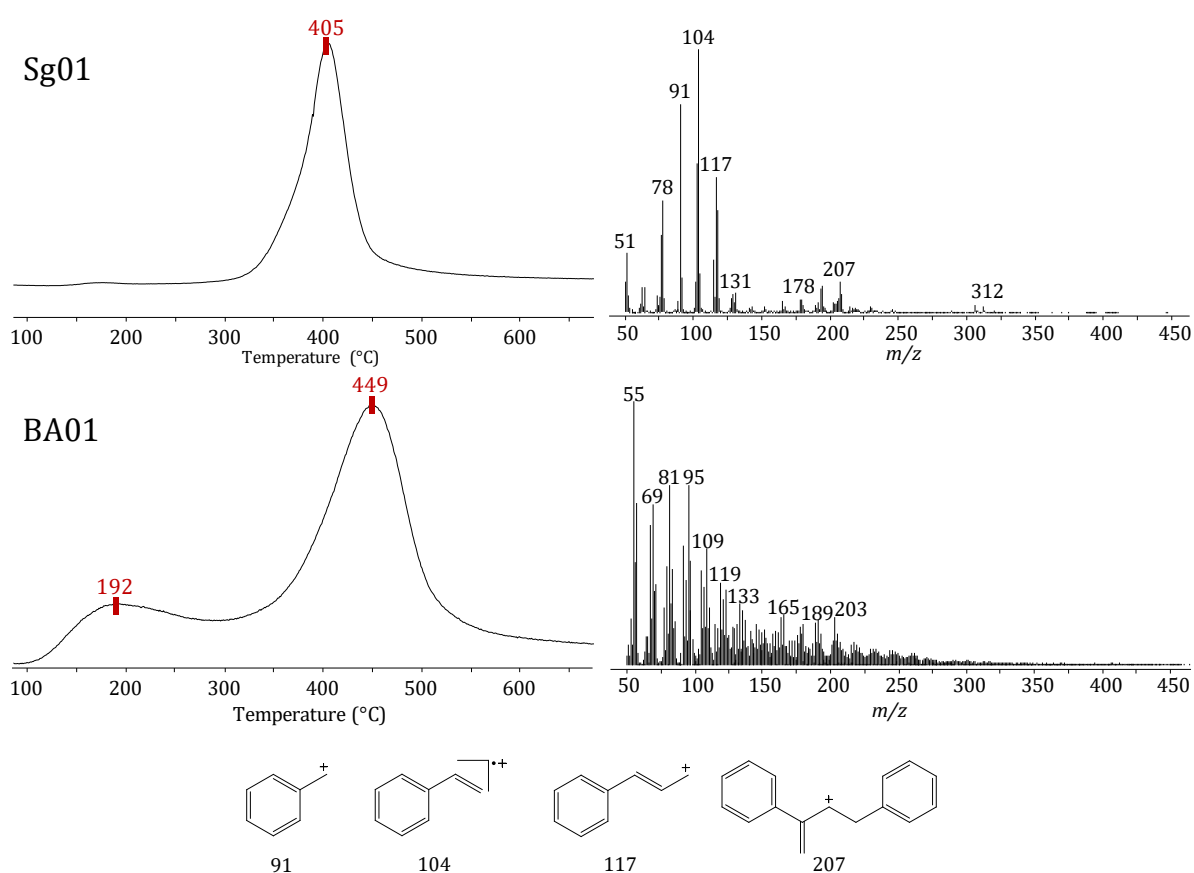
238 **3.2 Sieburgite and black ambers.** EGA-MS profiles for sample Sg01 and a representative
 239 black amber sample are shown in **Figure 2**. Sample Sg01 was the only instance of polystyrene-like
 240 amber in the sample pool. Polystyrene-like ambers belong to class III **of the Anderson system** [10,41].
 241 **This peculiar type of amber has been documented since the 19th century [42]. Grimaldi and co-workers**
 242 **gave a thorough account of polystyrene-like amber slabs found in New Jersey, but this type of amber**
 243 **was also found in the Bitterfeld deposit [43,44].**

244 The average mass spectrum for this sample showed the characteristic m/z signals ascribable to
 245 polystyrene [35]. The sample showed a single gas evolution region, with a signal peak at 405 °C. The
 246 high value for this signal peak indicates that the gas evolution peak corresponds to a thermal

247 degradation of the polymeric bulk of the material, and that sample Sg01 contains very small amounts
248 of non-polymeric species. While polystyrene represents the bulk of the sample, the presence of
249 oxygenated species in sieburgite has also been reported. These species are mainly cinnamic acid and
250 its esters, which have been proven to act as cross-linkers in the polymeric network [41]. ~~These~~
251 ~~compounds are most likely related to the original components of the resin. The most likely botanical~~
252 ~~origin for this amber is in fact the liquidambar plant (*Altingiaceae* family), whose resin has a high~~
253 ~~content of cinnamic acid and its esters [45]. Upon pyrolysis, these oxygenated species generate~~
254 ~~characteristic compounds~~ cinnamic acid derivatives such as 3-phenylpropanylcinnamate, which has
255 been proposed by Pastorova and co-workers as a marker to distinguish sieburgite from New Jersey
256 class III amber and from synthetic polystyrene, which could be used to produce fakes [41]. ~~whose~~The
257 mass spectrum of 3-phenylpropanylcinnamate shows a signal at m/z 118 as base peak. The relative
258 intensity of m/z 118 in sample Sg01 is indeed higher than what is usually observed for synthetic
259 polystyrene [32], ~~suggesting that this sample contains cinnamic acid and its esters.~~ However, m/z 118
260 can also be ascribed to methylstyrene, which is also a pyrolysis product of polystyrene [35]. Therefore,
261 no definitive conclusion ~~on the authenticity or the botanical origin of this sample~~ can be drawn on this
262 sample based on EGA-MS analyses alone.

263 Black amber is also known as stantienite [16]. Contrary to sieburgite, the EGA-MS profiles of all black
264 ambers showed two main gas evolution regions: a first region in the range 100 – 300 °C, and a second
265 region in the range 300 – 600 °C. Interpretation of the mass spectra of BA samples was not
266 straightforward, as the highest signals throughout the thermogram were at low m/z values (below
267 m/z 150), which are poorly diagnostic. However, three series of signals can be outlined, corresponding
268 to saturated (m/z 57, 71, 85), mono-unsaturated (m/z 55, 69, 83, 97, 111), and di-unsaturated (m/z
269 67, 81, 95, 109, 123) linear aliphatic hydrocarbons. These signals were present with little variations in
270 relative intensity throughout the EGA-MS profile, indicating that linear hydrocarbons are the main
271 components of both the ~~molecular and macromolecular~~ non-polymeric and polymeric fractions of
272 black ambers. This indicates that black ambers underwent extensive maturation, and are almost
273 completely fossilized.

274 Yamamoto and co-workers [16] identified two homolog series of methyl esters of mono- and
 275 dicarboxylic fatty acids in dichloromethane:methanol extracts of a stantienite sample. Both categories
 276 of compounds share m/z 74 as a very intense signal in their mass spectra. However, this signal was not
 277 found in any of the BA samples of our study, suggesting that our black amber samples are either at a
 278 more advanced state of maturation, or that their content of these methyl esters is extremely low. The
 279 amount of methyl esters in the stantienite sample of Yamamoto is not known, as no information is
 280 provided on the amount of sample used for the extraction.
 281



283 **Figure 2:** EGA-MS profiles and average mass spectra for samples Sg01 (siegburgite) and BA01
 284 (stantienite). Proposed structures of ions for m/z signals of relevance in sample Sg01 are also shown.

285

286 **3.3 Succinite, rumanite, gedanite and gedano-succinite.** EGA-MS profiles and average mass
 287 spectra for these four types of amber are presented in **Figure 3**. All Su, Ru, Ge and GS samples showed
 288 two gas evolution regions in the temperature ranges 100 – 300 °C and 300 – 550 °C. As observed for

289 the other amber types, these regions can be ascribed to desorption of ~~molecular~~ non-polymeric
290 compounds at low temperatures, and to the pyrolysis of the polymeric matrix above 300 °C. While this
291 behavior is shared by all samples, the two gas evolution regions displayed different profiles. For
292 instance, gedanites and gedano-succinites provided gas evolution regions with multiple signal peaks
293 both in the thermal desorption and the pyrolysis ranges, while most succinites and rumanites
294 provided a single peak in either range.

295 Interpretation of the mass spectra of these samples was based on the results of previous studies
296 dealing with succinite and rumanite [8,17,18,24], and on studies dealing with the interpretation of
297 mass spectra of diterpenes [36,37]. The thermal desorption region of all samples showed high signals
298 of m/z 95, 119 and 134. The signal at m/z 95 can be ascribed to camphene-like monoterpenoids, such
299 as borneol and camphor, ~~which~~ while those at m/z 119 and 134 can be ascribed to aromatic
300 monoterpenes such as *p*-cymene. ~~The main aromatic monoterpene found in succinite is *p*-cymene,~~
301 ~~whose structure is~~ Structures for these compounds are shown in **Figure 3**. All these compounds were
302 detected in the volatile fraction of rumanite and succinite samples by SPME [17]. ~~All-gedanite~~ Gedanite
303 and gedano-succinite samples showed additional signals at m/z 241, 257, 287, 302, with peaks at
304 approximately 240 °C. These signals can be ascribed to diterpenoid acids. A survey of the mass spectra
305 of diterpenoid acids available in the literature and in the NIST library showed that the abietane,
306 pimarane and isopimarane structures are the most likely to be present in Ge and GS samples. The
307 signal at m/z 302 corresponds to the molecular ion of abietic/pimaric/isopimaric acid, while the other
308 signals can be ascribed to ions obtained by characteristic fragmentation patterns, such as the loss of
309 methyl radical or decarboxylation.

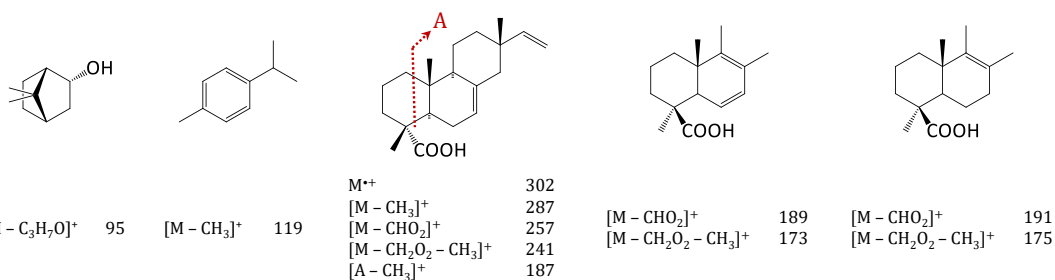
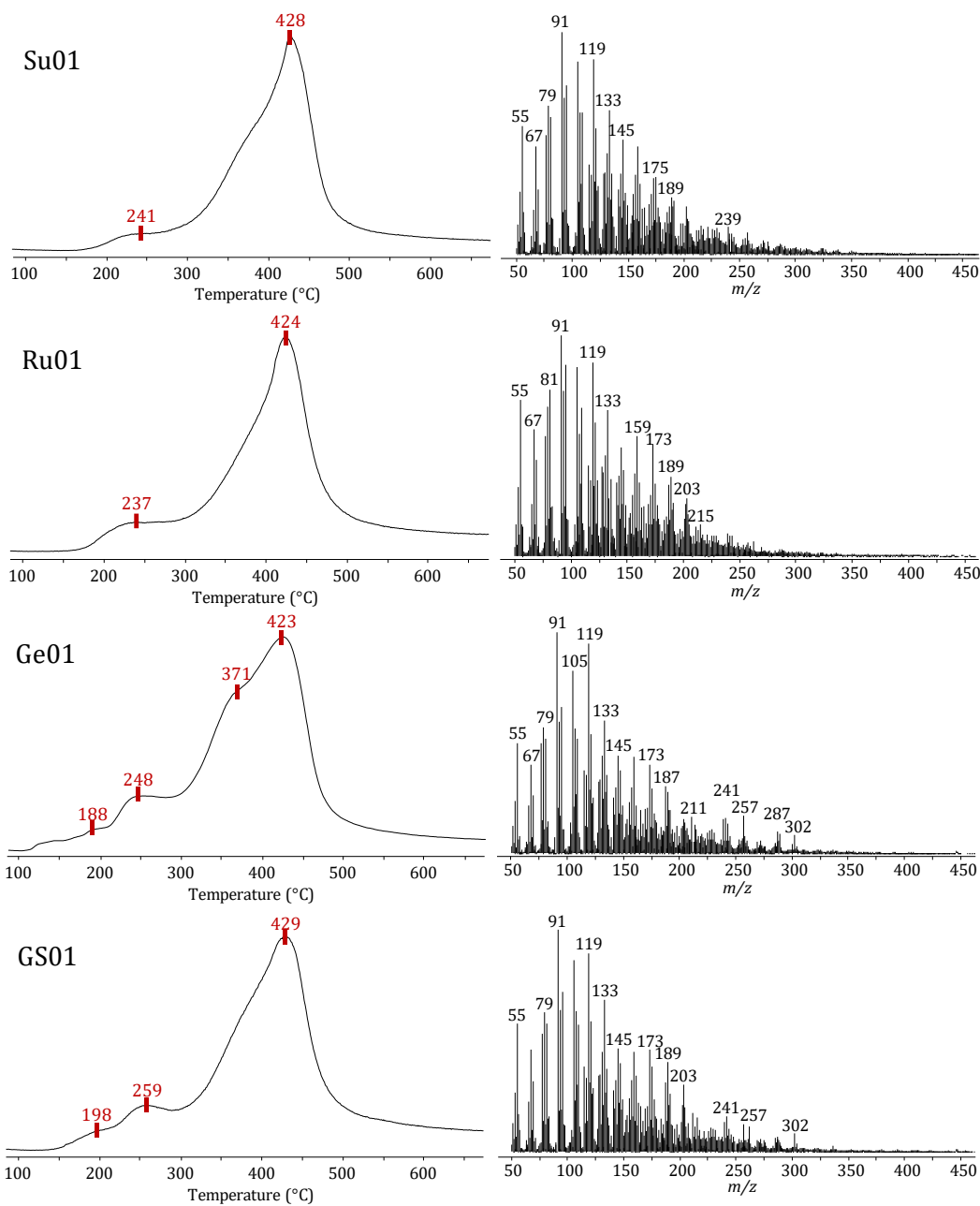
310 The second gas evolution region showed very complex mass spectra in all samples. Discussion of this
311 region of the thermogram is particularly challenging, as the signals with the highest intensities were at
312 relatively low m/z values, which are poorly diagnostic. Compared to the first gas evolution region,
313 higher relative intensities were observed for m/z 173, 175, 177, 189 and 191. These signals can be
314 ascribed to the bicyclic pyrolysis products of the poly-labdanoid polymeric network which is known to
315 be the main constituent of the bulk of succinite and rumanite ambers [8]. The same signals were found

316 in gedanite and gedano-succinite, indicating that these samples also share a similar composition of the
317 polymeric fraction. The mass spectra of both gas evolution regions demonstrate that Su, Ru, Ge and GS
318 samples all share very similar compositional profiles. This is in agreement with results available in the
319 literature, which ascribe all these amber varieties to a common botanical source [8,39], and allows us
320 to assign all ~~our~~ samples to class I ~~of the Anderson system~~. Class I contains a range of subclasses with
321 significantly different molecular composition. A pivotal discrimination criterion among these
322 subclasses is the presence and amount of succinic acid, which can be found for instance in subclass Ia,
323 and Id ambers, but not in subclasses Ib and Ic [6]. Succinic acid in amber can be found in amounts as
324 high as 8% [39], and can be both a component of the non-polymeric fraction, and part of the polymeric
325 matrix, forming ester bonds with hydroxy groups on polymerized terpenoids [46]. Free succinic acid
326 can be converted in the corresponding anhydride during heating [47,48]. However, both succinic acid
327 and succinic anhydride show high signals at low m/z values, which are poorly diagnostic as they can
328 also be ascribed to numerous fragmentations of the terpenoid components. Detection of the terpenoid-
329 succinic acid esters is also challenging, as their main fragment ions are the same of non-esterified
330 terpenoids [46]. Therefore, detection of succinic acid or its derivatives in EGA-MS profiles was not
331 possible, and we avoided assigning the samples to specific subclasses.

332 As Su, Ru, Ge and GS ambers all provided similar gas evolution profiles, principal component analysis
333 (PCA) was performed to highlight differences between the four types. Average mass spectra in the
334 range m/z 50 – 300 and 100 – 550 °C were used as data matrix. The results are presented in **Figure 4**.
335 The first two principal components accounted for approximately 75% of the total variance. The most
336 interesting discrimination of the samples was along the first principal component, in which all
337 rumanite samples were at negative values, and all succinite, gedanite and gedano-succinite samples
338 were at positive values. The loading plot of the first principal component, also shown in **Figure 4**,
339 indicates that m/z 55, 57, 69 and 83 are the main signals pulling samples towards negative values.
340 While not diagnostic, these m/z signals can be ascribed to small hydrocarbon fragment ions deriving
341 from the terpenes of both the ~~molecular and macromolecular~~ non-polymeric and polymeric fractions
342 of amber. The results of the PCA indicates that rumanite samples have higher relative intensities of

343 these signals. This suggests that rumanite has a higher content of defunctionalized terpenes, and a
344 lower content of oxygenated functional groups. This result is consistent with the findings of Stout and
345 co-workers [8], who identified rumanite as a variety of succinite amber which underwent a partial
346 thermal degradation, accelerating the maturation process of amber and favoring defunctionalization
347 and the loss of hydroxy and carboxy groups. Exposure to high temperatures also likely favored the loss
348 of low-molecular weight components from the bulk of the amber. This hypothesis is supported in our
349 results by the loading of m/z 119, which pulls samples towards positive values of the PC1. As m/z 119
350 can be ascribed to monoterpenes, the results of the PCA suggest that succinite, gedanite and gedano-
351 succinite samples have a higher content of low-molecular weight compounds than rumanite.
352 PCA was also repeated using average mass spectra obtained either from the thermal desorption region
353 (100 – 300 °C) or from the pyrolysis region (300 – 550 °C) of the thermogram. The resulting score and
354 loading plots are available in the Supplementary Material. Interestingly, both additional PCAs provided
355 very similar results to those obtained with the first one. This indicates that the compositional
356 differences between rumanite and succinite/gedanite/gedano-succinite involve both the ~~molecular~~
357 ~~and macromolecular~~ non-polymeric and polymeric fractions. When considering MS signals from the
358 thermal desorption region, a high load of m/z 119 was obtained pulling samples towards negative
359 values of PC1, and Su, Ge and GS samples were found at negative PC1 scores. This suggests that these
360 samples have a higher content of cymene-like monoterpenoids, which are the main responsible for the
361 signal at m/z 119 in the thermal desorption region. This is in agreement with the results obtained by
362 van der Werf and co-workers [17], in which PCA of SPME chromatograms also showed that Baltic
363 amber contains more cymene terpenoids than rumanite.
364 Note that succinite, gedanite and gedano-succinite could not be separated from each other, even along
365 the other principal components. This indicates that the compositional differences between these three
366 types of amber are small in comparison with the differences from rumanite samples. We avoided
367 repeating PCA on Su, Ge and GS ambers as the number of samples is not sufficient to draw statistically
368 significant conclusions. To attempt discrimination of gedanite and gedano-succinite, principal

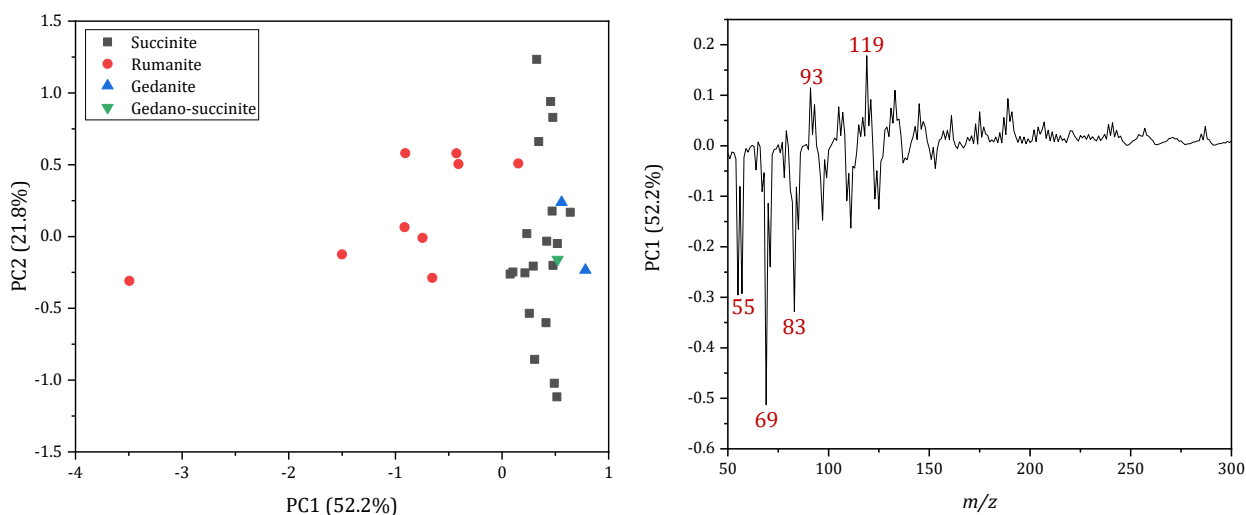
369 component analysis was also repeated using normalized total ion profiles instead of the average mass
370 spectra, but no further discrimination was obtained.
371



372

373 **Figure 3:** EGA-MS profiles and average mass spectra for samples Su01 (succinite), Ru01 (rumanite),
 374 Ge01 (gedanite) and GS01 (gedano-succinite). Proposed structures of ions for m/z signals of relevance
 375 are also shown.

376



377

378 **Figure 4:** Left – Score plot of the first two principal components of all Su, Ru, Ge and GS samples. Right
 379 – Loading plot of the first principal component.

380

381 **3.4. Italian ambers.** EGA-MS profiles for samples Si01 and CI01-03 are shown in **Figure 5**.

382 Sicilian amber has been documented in a previous study by van der Werf and co-workers [38]. Py-
 383 GC/MS analysis of this amber provided mostly diterpenes with the enantio-biformene carbon skeleton,
 384 as well as bicyclic compounds deriving from the pyrolysis of these diterpenes. The characteristic m/z
 385 signals of these compounds were also detected in the mass spectra of both simetite samples in this
 386 study. High relative intensities of m/z 245 and 260 were observed in the thermal desorption region.
 387 These signals can be ascribed to **biformene-like diterpenes with 19 carbon atoms, which were found in**
 388 **significant amounts in the study by van der Werf and co-workers. The most abundant biformenes**
 389 **found in the study by Werf and co-workers display a saturated aliphatic chain with a terminal carboxy**
 390 **group. The structure A representative structure** for one of these compounds is shown in **Figure 5**.
 391 **Note that m/z 245 and 260 correspond to decarboxylated forms of this compound. The same signals**
 392 **could be obtained from biformene structures with no functional groups.** Interestingly, the relative
 393 intensity of m/z 119 in these samples was lower than those observed in the other diterpenoid ambers,
 394 indicating a low content of aromatic monoterpenes.

395 Pyrolysis of the polymeric fraction of Sicilian ambers showed very similar signals to those observed

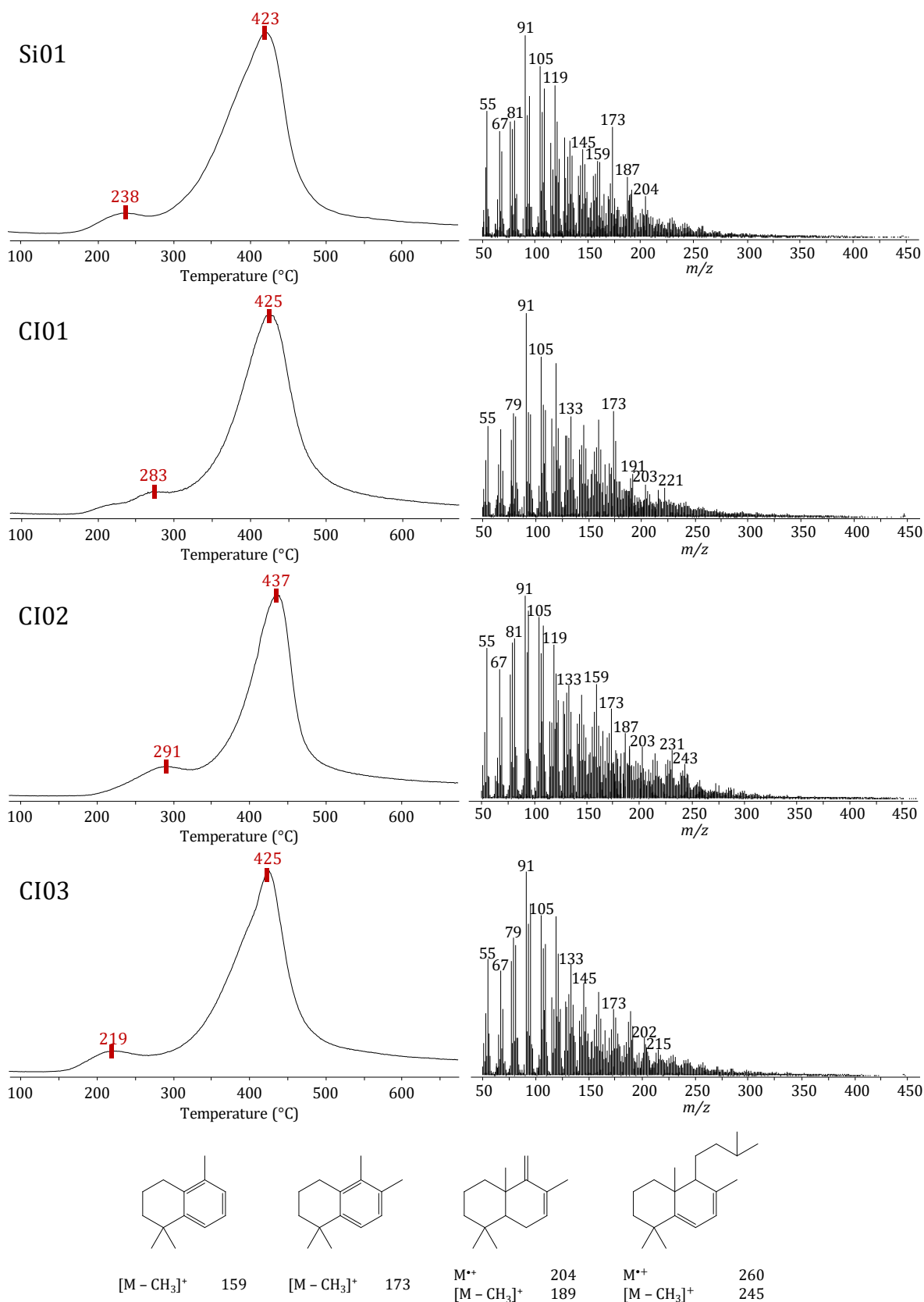
396 for the ambers described in Section 3.3, leading us to the conclusion that the macromolecular network

397 is mainly constituted of polymeric labdane terpenoids. Based on the findings of van der Werf [38], we
398 can hypothesize that this polymeric network is most likely composed of biformene-like labdane,
399 reflecting the composition of the non-polymerized fraction. These results allowed us to conclude that
400 Sicilian ambers can also be ascribed to class I of the Anderson system. More specifically, we can
401 hypothesize that these samples belong to class Ic, due to the presence of *enantio*-biformene
402 terpenoids, but confirmation of this hypothesis would require chromatographic separation of the
403 pyrolysis products.

404 Samples CI01-03 were obtained from central Italy. A single literature reference is available for these
405 samples, in which characterization was performed by infrared spectroscopy [49], but no references
406 were found reporting mass spectral data. Therefore, interpretation of their mass spectra was based on
407 the results obtained for the other samples. The main differences in these samples were found within
408 the thermal desorption region of their gas evolution profiles. Sample CI01 showed a very high signal of
409 m/z 119, indicating the presence of free aromatic monoterpenes such as cymene. On the other hand,
410 while samples CI02 and CI03 showed high signal intensity at m/z 95. This m/z value was not observed
411 for other samples, but it can be ascribed to monoterpenes with the bornane or camphene carbon
412 skeleton, such as borneol and camphor. Additional signals can be found that could be ascribed to
413 monoterpenes, such as m/z 109 in CI02 and m/z 121 in CI03. Two literature studies are available
414 describing ambers from this region [31,49], including a work by van der Werf in which Py-GC/MS was
415 performed on a sample with the same geological origin as sample CI03. As most of the other samples,
416 CI ambers showed two thermal degradation regions. In the first region, all samples showed high
417 signals at m/z 119, 159, and 173. Samples CI02 and CI03 also showed high intensities of m/z 95.
418 Signals at m/z 95 and 119 can be ascribed to fragment ions of octahydronaphthalenes, while signals at
419 m/z 159 and 173 can be ascribed to tetrahydronaphthalenes with one aromatic and one aliphatic ring.
420 These species are found in class I ambers as a result of defunctionalization and loss of the aliphatic
421 side-chain of labdanoid diterpenes [50]. Octahydronaphthalenes were indeed found in the study by
422 van der Werf [31]. Representative structures of tetrahydro- and octahydronaphthalenes are shown in
423 **Figure 5** to account for these signals. These structures have been chosen among those detected in Py-

424 ~~GC/MS of other diterpenoid ambers [17,18]. As monoterpenes are highly volatile compounds, their~~
425 ~~presence suggests that these samples are less mature than the other ambers analyzed in this study.~~
426 Sample CI02 also showed the same signals at m/z 245 and 260 that were found in the Sicilian ambers.
427 This led us to the conclusion that sample CI02 is also constituted of biformene terpenoids. A high
428 relative intensity was also observed for m/z 231 in CI02. While this signal is not characteristic of
429 biformene-like terpenoids, unidentified compounds with this signal were detected in Py-GC/MS of
430 Sicilian amber [38].
431 Finally, all three samples provided very similar mass spectra in the pyrolysis region. These mass
432 spectra were like those obtained for Sicilian ambers and the other diterpenoid ambers, suggesting the
433 presence of a labdanoid-based polymeric network. For this reason, all CI samples were also ascribed to

434 class I ~~of the Anderson system~~. This also agrees with the results obtained by van der Werf [31].



435

436 **Figure 5:** EGA-MS profiles and average mass spectra for samples Si01 (simeite) and CI01-03 (ambers

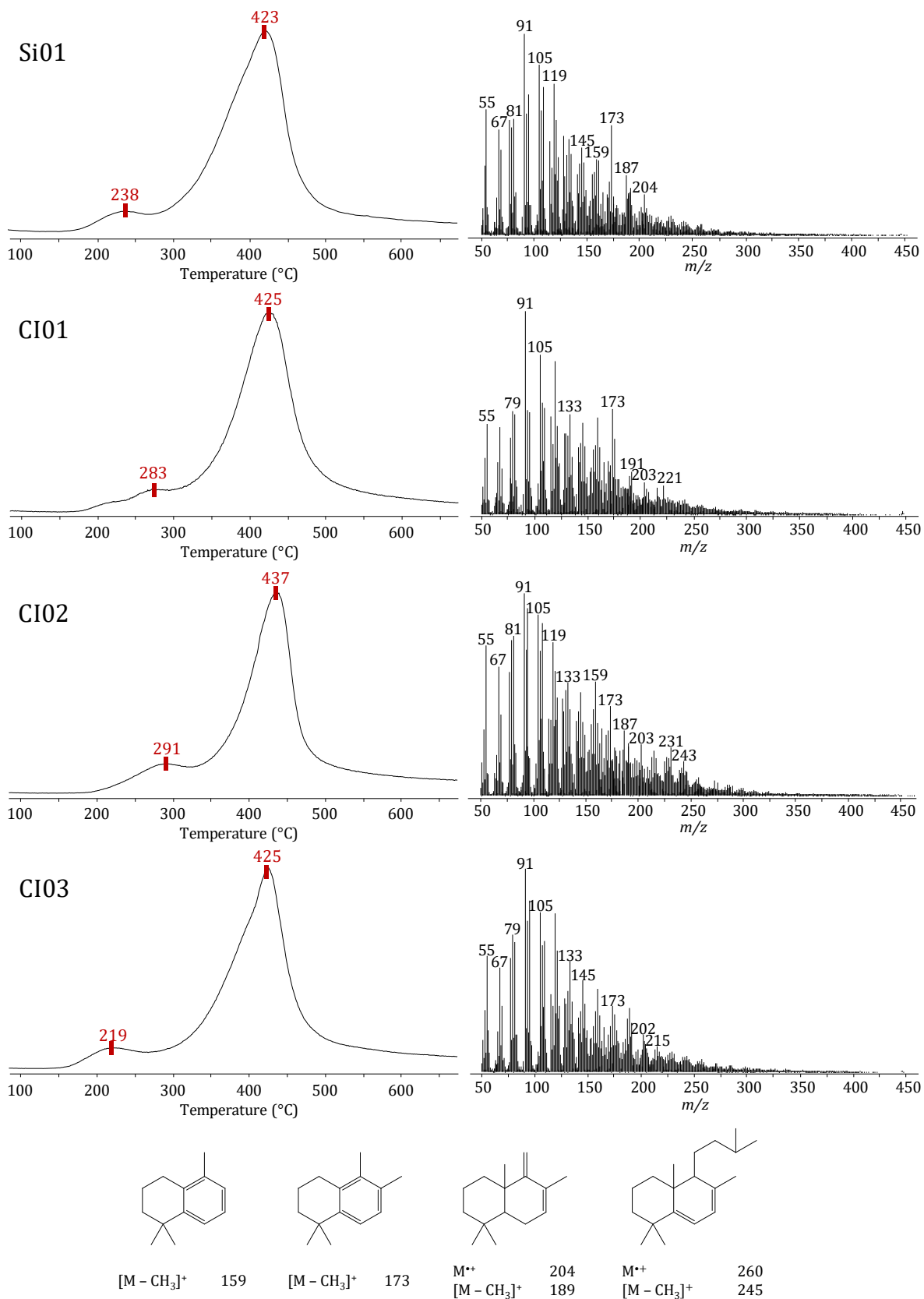
437 from central Italy). Proposed structures of ions for m/z signals of relevance are also shown.

438

439 **Table 2** **Table 2** provides a synthetic report of the ~~Anderson~~ classes and main components of both

440 ~~molecular non-polymeric~~ and polymeric fractions for all amber samples in this study.

441



442

443 **Figure 5:** EGA-MS profiles and average mass spectra for samples Si01 (simetite) and CI01-03 (ambers

444 from central Italy). Proposed structures of ions for m/z signals of relevance are also shown.

445

446 **Table 2:** ~~Anderson-class~~ Classes and composition of the ~~molecular and macromolecular~~ non-polymeric
 447 and polymeric fractions of all amber samples in this study, based on EGA-MS results.

Amber type	Class	Molecular Non-polymeric fraction (< 300 °C)	Polymeric fraction (> 300 °C)
Glessite	II	Cadinene-like sesquiterpenes Ursane/oleanane-like triterpenes	Polymeric cadinenes
Goitschite	II	Cadinene-like sesquiterpenes Ursane/oleanane-like triterpenes with methyl-carboxylates on C28	Polymeric cadinenes
Sieburgite	III	-	Polystyrene, possibly with oxygenated cross-linkers
Black amber	-	Aliphatic hydrocarbons	Aliphatic hydrocarbons
Succinite	I	Aromatic monoterpenoids Camphene-like monoterpenoids Cymene-like monoterpenoids	Polylabdene
Rumanite	I	Aromatic monoterpenoids Camphene-like monoterpenoids Cymene-like monoterpenoids	Polylabdene
Gedanite	I	Aromatic monoterpenoids Camphene-like monoterpenoids Cymene-like monoterpenoids Pimarane-like diterpenoid acids	Polylabdene
Gedano-succinite	I	Aromatic monoterpenoids Pimarane-like diterpenoid acids	Polylabdene
Simetite	I	Biformene-like diterpenoids	Polylabdene (likely based on enantio-biformene)
CI01	I	Aromatic monoterpenoids Tetrahydronaphthalenes	Polylabdene
CI02	I	Bornane/camphene-like monoterpenoids Tetrahydronaphthalenes Octahydronaphthalenes Biformene-like diterpenoids	Polylabdene
CI03	I	Bornane/camphene-like monoterpenoids Tetrahydronaphthalenes Octahydronaphthalenes	Polylabdene

448

449

450 4. CONCLUSIONS

451 Gas evolution profiles of almost all ambers showed two main regions, which could be ascribed to the
452 desorption of low-molecular weight compounds at low temperatures, and to the pyrolysis of the
453 polymeric network above 300 °C. ~~Samples with different geological origin generally showed different
454 desorption/pyrolysis temperatures and different number of desorption peaks, highlighting the
455 usefulness of EGA-MS in providing information for the development of Py-GC/MS experiments
456 targeting different fractions of specific amber samples. The results agree with previous literature
457 studies and show that EGA-MS can be used to obtain information on both the molecular and
458 macromolecular fractions of geological amber samples with different compositions and geographical
459 origins. EGA-MS profiles could be used to differentiate between two types of class II ambers, glessite
460 and goitschite, based on the different constituting triterpenoids. Distinction of succinite and rumanite
461 ambers was also possible by principal component analysis of their average mass spectra.
462 The results obtained for ambers with documented molecular compositions were also used to
463 characterize three previously unreported amber samples deriving from central Italy. This
464 demonstrates that EGA-MS analyses can be used not only to evaluate the content of molecular and
465 macromolecular components of ambers with known composition, but also to characterize ambers with
466 unknown origin.~~

467 EGA-MS provided valuable information on the thermal behavior of all amber samples, and on their
468 content of non-polymeric and polymeric components. The results ~~could be used~~ allowed us to
469 attribute a class to most of the samples. These classes were in agreement with those attributed in
470 previous literature studies dealing with ambers with same geological origins, with the only exception
471 of the goitschites, which were identified as triterpenoid ambers and not diterpenoid. ~~to assign most of
472 the samples to an Anderson class. However, further classification was not possible~~ The two types of
473 class II ambers, glessite and goitschite, could be distinguished based on the different constituting
474 triterpenoids. Distinction of succinite and rumanite samples was also possible by principal component
475 analysis of their average mass spectra.

476 For ambers of class I, subclasses could not be attributed due to the inability to detect the presence of
477 succinic acid or to pinpoint specific terpenoid structures. Succinic acid is a minor component of amber
478 at best, with a net content of 8% in the richest samples. In addition, the mass spectrum of succinic acid
479 only presents high signals at low m/z values, which are difficult to isolate from the signals of all other
480 components in the complex mass spectra. This means that, while EGA-MS can provide valuable
481 information on the thermal degradation profile of an amber sample, other techniques such as Py-
482 GC/MS or spectroscopic techniques should also be used to obtain a complete picture of the molecular
483 composition. This highlights a limitation of EGA-MS results, which is the lack of chromatographic
484 separation of the desorption/pyrolysis products. For this reason, additional characterization with Py-
485 GC/MS or spectroscopic techniques should be performed on the sample pool. A particularly promising
486 approach would be the use of step-wise Py-GC/MS, which could be achieved by sequentially heating an
487 amber sample at two different temperatures, in order to achieve the desorption of the molecular non-
488 polymeric fraction, followed by the pyrolysis of the residual polymeric fraction. For such a study, the
489 choice of desorption/pyrolysis temperatures would be guided by the EGA-MS results obtained in this
490 work.

491

492 **ACKNOWLEDGEMENTS**

493 The Authors are deeply grateful to all the institutions for providing the amber samples.

494

495 **REFERENCES**

- 496 [1] D.A. Grimaldi, *Amber in Nature*, in H. Whelcher (Ed.), *Amber - Window to the Past*, Harry N.
497 Abrams, Incorporated, New York, USA, 1996, p. 11.
- 498 [2] S. Veil, K. Breest, P. Grootes, M.-J. Nadeau and M. Hüls, A 14 000-year-old amber elk and the origins
499 of northern European art; *Antiquity* 86 (2012) 660.
- 500 [3] M.P. Colombini, E. Ribechini, M. Rocchi and P. Selleri, Analytical pyrolysis with in-situ silylation,
501 Py(HMDS)-GC/MS, for the chemical characterization of archaeological and historical amber objects;
502 *Heritage Science* 1 (2013) 6.
- 503 [4] R. Shor, The History and Reconstruction of the Amber Room; *Gems & Gemology* 54 (2018) 378.
- 504 [5] D.J. Clifford, P.G. Hatcher, R.E. Botto, J.V. Muntean, B. Michels and K.B. Anderson, The nature and
505 fate of natural resins in the geosphere—VIII.1 For the last publication in this series see Anderson,
506 1996.1 NMR and Py–GC–MS characterization of soluble labdanoid polymers, isolated from
507 Holocene class I resins; *Organic Geochemistry* 27 (1997) 449.
- 508 [6] K.B. Anderson and J.C. Crelling, *Introduction*, in K.B. Anderson and J.C. Crelling (Eds.), *Amber,*
509 *Resinite, and Fossil Resin*, American Chemical Society, USA, 1995, p. XI.
- 510 [7] K.B. Anderson, R.E. Winans and R.E. Botto, The nature and fate of natural resins in the geosphere—
511 II. Identification, classification and nomenclature of resinites; *Organic Geochemistry* 18 (1992) 829.
- 512 [8] E.C. Stout, C.W. Beck and K.B. Anderson, Identification of rumanite (Romanian amber) as thermally
513 altered succinite (Baltic amber); *Physics and Chemistry of Minerals* 27 (2000) 665.
- 514 [9] M.A. Wilson, J.V. Hanna, K.B. Anderson and R.E. Botto, 1H CRAMPS NMR derived hydrogen
515 distributions in various coal macerals; *Organic Geochemistry* 20 (1993) 985.
- 516 [10] W. Winkler, M. Musso and E.C. Kirchner, Fourier transform Raman spectroscopic data on the fossil
517 resin siegburgite; 34 (2003) 157.
- 518 [11] J.B. Lambert and G.O. Poinar, Amber: the Organic Gemstone; *Accounts of Chemical Research* 35
519 (2002) 628.
- 520 [12] A.P. Wolfe, R.C. McKellar, R. Tappert, R.N.S. Sodhi and K. Muehlenbachs, Bitterfeld amber is not
521 Baltic amber: Three geochemical tests and further constraints on the botanical affinities of
522 succinite; *Review of Palaeobotany and Palynology* 225 (2016) 21.
- 523 [13] C.W. Beck, Spectroscopic Investigations of Amber; *Applied Spectroscopy Reviews* 22 (1986) 57.
- 524 [14] E. Ragazzi, G. Roghi, A. Giaretta and P. Gianolla, Classification of amber based on thermal analysis;
525 *Thermochemica Acta* 404 (2003) 43.
- 526 [15] M. Feist, I. Lamprecht and F. Müller, Thermal investigations of amber and copal; *Thermochemica*
527 *Acta* 458 (2007) 162.
- 528 [16] S. Yamamoto, A. Otto, G. Krumbiegel and B.R.T. Simoneit, The natural product biomarkers in
529 succinite, glessite and stantienite ambers from Bitterfeld, Germany; *Review of Palaeobotany and*
530 *Palynology* 140 (2006) 27.
- 531 [17] I.D. van der Werf, A. Aresta, G.I. Truică, G.L. Radu, F. Palmisano and L. Sabbatini, A quasi non-
532 destructive approach for amber geological provenance assessment based on head space solid-
533 phase microextraction gas chromatography–mass spectrometry; *Talanta* 119 (2014) 435.
- 534 [18] K.B. Anderson and R.E. Winans, Nature and fate of natural resins in the geosphere. I. Evaluation of
535 pyrolysis-gas chromatography mass spectrometry for the analysis of natural resins and resinites;
536 *Analytical Chemistry* 63 (1991) 2901.
- 537 [19] K.B. Anderson and R.E. Botto, The nature and fate of natural resins in the geosphere—III. Re-
538 evaluation of the structure and composition of Highgate Copalite and Glessite; *Organic*
539 *Geochemistry* 20 (1993) 1027.
- 540 [20] J. Poulin and K. Helwig, The characterisation of amber from deposit sites in western and northern
541 Canada; *Journal of Archaeological Science: Reports* 7 (2016) 155.
- 542 [21] J. Poulin and K. Helwig, Class Id resinite from Canada: A new sub-class containing succinic acid;
543 *Organic Geochemistry* 44 (2012) 37.
- 544 [22] O.O. Sonibare, T. Hoffmann and S.F. Foley, Molecular composition and chemotaxonomic aspects of
545 Eocene amber from the Ameki Formation, Nigeria; *Organic Geochemistry* 51 (2012) 55.

- 546 [23] J.B. Lambert, J.A. Santiago-Blay and K.B. Anderson, Chemical Signatures of Fossilized Resins and
547 Recent Plant Exudates; 47 (2008) 9608.
- 548 [24] M. Vîrgolici, C. Ponta, M. Manea, D. Neguț, M. Cutrubinis, I. Moise, R. Șuvăilă, E. Teodor, C. Sârbu
549 and A. Medvedovici, Thermal desorption/gas chromatography/mass spectrometry approach for
550 characterization of the volatile fraction from amber specimens: A possibility of tracking geological
551 origins; *Journal of Chromatography A* 1217 (2010) 1977.
- 552 [25] F. Nardella, M. Mattonai and E. Ribechini, Evolved gas analysis-mass spectrometry and
553 isoconversional methods for the estimation of component-specific kinetic data in wood pyrolysis;
554 *Journal of Analytical and Applied Pyrolysis* 145 (2020) 104725.
- 555 [26] A. Bonini, F.M. Vivaldi, E. Herrera, B. Melai, A. Kirchhain, N.V.P. Sajama, M. Mattonai, R. Caprioli, T.
556 Lomonaco, F.D. Francesco and P. Salvo, A Graphenic Biosensor for Real-Time Monitoring of Urea
557 During Dialysis; *IEEE Sensors Journal* 20 (2020) 4571.
- 558 [27] M. Mattonai, A. Watanabe and E. Ribechini, Characterization of volatile and non-volatile fractions
559 of spices using evolved gas analysis and multi-shot analytical pyrolysis; *Microchemical Journal* 159
560 (2020) 105321.
- 561 [28] T. Nacci, F. Sabatini, C. Cirrincione, I. Degano and M.P. Colombini, Characterization of textile fibers
562 by means of EGA-MS and Py-GC/MS; *Journal of Analytical and Applied Pyrolysis* 165 (2022) 105570.
- 563 [29] K. Mänd, K. Muehlenbachs, R.C. McKellar, A.P. Wolfe and K.O. Konhauser, Distinct origins for Rovno
564 and Baltic ambers: Evidence from carbon and hydrogen stable isotopes; *Palaeogeography,
565 Palaeoclimatology, Palaeoecology* 505 (2018) 265.
- 566 [30] J.H. Langenheim, Plant Resins; *American Scientist* 78 (1990) 16.
- 567 [31] I.D. van der Werf, A. Monno, D. Fico, G. Germinario, G.E. De Benedetto and L. Sabbatini, A multi-
568 analytical approach for the assessment of the provenience of geological amber: the collection of
569 the Earth Sciences Museum of Bari (Italy); *Environmental Science and Pollution Research* 24 (2017)
570 2182.
- 571 [32] J. Karliner and C. Djerassi, Terpenoids. LVII. Mass Spectral and Nuclear Magnetic Resonance Studies
572 of Pentacyclic Triterpene Hydrocarbons; *The Journal of Organic Chemistry* 31 (1966) 1945.
- 573 [33] H. Budzikiewicz, J.M. Wilson and C. Djerassi, Mass spectrometry in structural and stereochemical
574 problems. XXXII. Pentacyclic Triterpenes; *Journal of the American Chemical Society* 85 (1963) 3688.
- 575 [34] B.G.K. Van Aarssen, J.W. de Leeuw, M. Collinson, J.J. Boon and K. Goth, Occurrence of polycadinene
576 in fossil and recent resins; *Geochimica et Cosmochimica Acta* 58 (1994) 223.
- 577 [35] S. Tsuge, H. Ohtani and C. Watanabe, *Pyrolysis-GC/MS data book of synthetic polymers: pyrograms,
578 thermograms and MS of pyrolyzates*, Elsevier, 2011, pp.
- 579 [36] T.-L. Chang, T.E. Mead and D.F. Zinkel, Mass spectra of diterpene resin acid methyl esters; 48
580 (1971) 455.
- 581 [37] H. Audier, S. Bory, M. Fetizon and N.-T.J.B.d.l.s.c.d.F. Anh, Spectres de masse de terpenes. 3.
582 Influence des liaisons ethyleniques sur la fragmentation des diterpenes; (1966) 4002.
- 583 [38] I.D. van der Werf, D. Fico, G.E. De Benedetto and L. Sabbatini, The molecular composition of Sicilian
584 amber; *Microchemical Journal* 125 (2016) 85.
- 585 [39] E.C. Stout, C.W. Beck and B. Kosmowska-Ceranowicz, *Gedanite and Gedano-Succinite*, in K.B.
586 Anderson and J.C. Crelling (Eds.), *Amber, Resinite, and Fossil Resins*, American Chemical Society,
587 USA, 1995, p. 130.
- 588 [40] S.A. Stout, *Resin-Derived Hydrocarbons in Fresh and Fossil Dammar Resins and Miocene Rocks and
589 Oils in the Mahakam Delta, Indonesia*, in *Amber, Resinite, and Fossil Resins*, American Chemical
590 Society, 1996, Chapter 3, p. 43.
- 591 [41] I. Pastorova, T. Weeding and J.J. Boon, 3-Phenylpropanylcinnamate, a copolymer unit in Siegburgite
592 fossil resin: a proposed marker for the Hammamelidaceae; *Organic Geochemistry* 29 (1998) 1381.
- 593 [42] H. Klinger and R. Pitschki, Ueber den Siegburgit; *Berichten der Deutschen Chemischen Gesellschaft
594 zu Berlin* 17 (1884) 2742.
- 595 [43] D.A. Grimaldi, C.W. Beck and J.J. Boon, Occurrence, chemical characteristics, and paleontology of
596 the fossil resins from New Jersey; *American Museum Novitates* 2948 (1989) 1.

- 597 [44] B.K. Kosmowska-Ceranowicz, G., Bursztyn Bitterfeldski (saksonski) i inne żywice kopalne z okolic
598 Halle; *Przeład Geologiczny* 9 (1990) 394.
- 599 [45] M. Hovaneissian, P. Archier, C. Mathe, G. Culioli and C. Vieillescazes, Analytical investigation of
600 styrax and benzoin balsams by HPLC- PAD-fluorimetry and GC-MS; 19 (2008) 301.
- 601 [46] J. Poulin and K. Helwig, Inside Amber: The Structural Role of Succinic Acid in Class Ia and Class Id
602 Resinite; *Analytical Chemistry* 86 (2014) 7428.
- 603 [47] G.C. Galletti and R. Mazzeo, Pyrolysis/gas chromatography/mass spectrometry and Fourier-
604 transform infrared spectroscopy of amber; 7 (1993) 646.
- 605 [48] A.M. Shedrinsky, T.P. Wampler and K.V. Chugunov, The examination of amber beads from the
606 collection of the state hermitage museum found in Arzhan-2 burial memorial site; *Journal of*
607 *Analytical and Applied Pyrolysis* 71 (2004) 69.
- 608 [49] I. Angelini and P. Bellintani, Archaeological ambers from northern Italy: an FTIR-DRIFT study of
609 provenance by comparison with the geological amber database; *Archaeometry* 47 (2005) 441.
- 610 [50] K.B. Anderson, *New Evidence Concerning the Structure, Composition, and Maturation of Class I*
611 *(Polylabdanoid) Resinites*, in K.B. Anderson and J.C. Crelling (Eds.), *Amber, Resinite, and Fossil*
612 *Resins*, American Chemical Society, USA, 1995, p. 105.

613